Design of 2D Photonic Crystal Biosensor to Detect Blood Components

Fariborz Parandin (fparandin@yahoo.com)
Razi University, Kermanshah, Iran https://orcid.org/0000-0001-9044-3048
farsad heidari
Islamic Azad University Branch of Kermanshah
Mehdi Aslinezhad
Shahid Sattari University of Aeronautical Engineering
Sobhan Roshani
Islamic Azad University Branch of Kermanshah
Saeed Roshani
Islamic Azad University Branch of Kermanshah

Research Article

Keywords: Photonic Crystal Biosensor, PBG, Band Structure

Posted Date: April 5th, 2022

DOI: https://doi.org/10.21203/rs.3.rs-1459722/v1

Abstract

Photonic crystals are periodic structures made of insulators. They are the best option to design biosensors. In this paper, a photonic crystal biosensor containing insulation rods in the air was designed and simulated. This biosensor was used as a photonic crystal circular nano-ring between the internal and external waveguides. At the end of the internal waveguide, a defect exists to create an increase in the coupling distance. This causes the quality factor and resonant wavelength displacement to increase. The purpose of designing this sensor is to check blood ingredients. After connecting to a measuring rod, this sensor shows different refractive indices. Another important characteristic of the proposed structure is that mostly radiuses of dielectric rods are identical. This causes the sensor construction to be easy. The plane-wave expansion (PWE) method is utilized to calculate the band structure. The results show that a photonic band gap (PBG) with a wavelength from 1.26 μm to 1.92 μm is created in this distance where no wavelength can spread.

1. Introduction

A photonic crystal is a structure that its refractive index changes alternatively, and this change can be one-, two-, and three-dimensional. Indeed, these structures are dual semiconductor crystals and influence the photons movement. The photonic crystals are alternative micro-nano structures of dielectric, which influence the pathway of the electromagnetic wave. This function is very similar to the alternative potential, which influences electrons to move with the creation of forbidden and permitted energy bands in semiconductors. The base function of these crystals is based on the internal alternative change of the refractive index in the crystal. Comparing other existing photonic structures, photonic crystal structures have a better optical limitation. This optical limitation is created due to the photonic band gap, which exists in all directions of the alternative structure. In a photonic crystal structure, this gap includes frequencies on which electromagnetic waves are not allowed to spread. In a photonic crystal structure, insulation materials with low loss can be used to control the spread of electromagnetic waves in some directions, especially with certain frequencies [1]. Photonic crystals have many capabilities in designing optical circuits. One of their applications is in digital circuits, so that they can be used in the design of logic gates [2–7], comparators [8–9], adders, subtractors [10–13], decoders, encoders [14–17] and other logic circuits.

Nowadays, the importance of analyzing different cases such as clinical diagnosis, biomedical research, medical health, nano, forensic medicine, and food are increasing. For this purpose, so far, different biosensors were designed and implemented [18–28]. A biosensor was designed such that only responses to a special substance, and the consequence of this reaction is the messages and signals sent to the processing part. Each biosensor totally has two parts: receiver and converter. The main job of the bio-receiver is to detect analyte interactions. On the other hand, the converter converts these detections and reactions to signals that can measure them until the function is performed easily [29–30]. The biosensor is described as a set of means which usually detect the interest substance in electrical, optical, and thermal forms using special biochemical reactions mediated by isolated enzymes, tissues, cells, or any

chemical elements. These sensors are many applications. For example, we can mention the following uses such as in very small devices embedded in the human body, chemical and biological wars, pesticides, and harmful bacteria.

According to the technological progress in electronics areas and decrease in dimensions of the relevant device, a tendency towards micro-sensors and nano-sensors are becoming more and more. One of the best options is photonic crystal biosensors [31–35].

In [36], a biosensor was designed based on a circular resonant nano-ring between upper and lower waves. Several insulation rods have been displaced and lied on near each other to increase the optical limitation. In [37], a biosensor based on insulation rods in the air was presented. In this structure, an ellipse-shaped nano-ring has been embedded between the waveguide in output and input. An insulation rod was located between the internal waveguide and nano-ring to increase optical coupling and quality factor. In [38], a biosensor based on one-dimensional photonic crystal defects was presented. In this sensor, the biosensor function was studied using the Trimmed Mean of the M-values (TMM) approach. The outcome parameters can obtain the concentration of Creatine in blood, the thickness of the violation layer, etc.

In [39], a biosensor based on the air cavities was presented in a silicon plate. This sensor was constructed from the defects in the form of a capsule between two waveguides. These capsule defects lie at the center of this structure. This sensor was designed to detect glucose concentration in the human body.

In [40], a one-dimensional photonic crystal biosensor was presented to detect blood plasma and cancer cells. The interest structure was constructed from lying on a compressed layer between two identical photonic crystal structures of Silica and Titanium.

A photonic crystal biosensor was studied and analyzed. The interest structure includes photonic crystal insolation rods in the air platform. Hence, blood ingredients are reviewed and obtained by connecting the desired biomolecules to measure rods of the biosensor structure, refractive index, sensitivity, and other parameters of each desired substances.

2. Photonic Crystal Biosensors

Photonic crystal structures have a better optical limitation than other optical devices, and they can limit light to a special place and be resistant to electromagnetic interference. A measure of biosensors is based on the focus of an electrical field on a region with a low refractive index. This causes the sensitivity of the biosensor to increase and the smallest change in the refractive index to be detected. The photonic crystal biosensors are easily able to be integrated due to having a small measure area. In the biosensors based on photonic crystals, the measurable parameter is identified using the change analysis of the refractive index in the photonic crystal structure [26].

There are multiple important parameters in the biosensors that are the base mechanisms for the assessment and measurement of this kind of sensors [32]. Of the most important parameters in photonic

crystal sensors is the quality factor which is given as follows (Eq. 1):

(1) $Q = \frac{\lambda_0}{\Delta\lambda_{FWHM}}$

where λ is a central resonant wavelength, and $\Delta\lambda_{FWHM}$ is the spectral width of half maximum for the central transmission spectrum.

Another parameter of biosensors is sensitivity. The sensitivity is the level of a change in passing a signal at a biosensor in response to analyte connection change in a sensing hole. It is defined as follows (Eq. 2).

$$\mathrm{s} = \frac{\Delta\lambda}{\Delta n}$$

(2)

where $\Delta\lambda$ is the transmission spectrum displacement and Δn is the refractive index changes.

Another important parameter is the detection limit which is obtained as follows (Eq. 3).

$$\mathrm{DL} = \frac{\lambda}{10SQ}$$

(3)

where λ is a resonant wavelength, S is the sensitivity, and Q is the quality factor.

The next parameter is the figure of merit (FOM) which is determined as following (Eq. 4).

$$\mathrm{FOM} = \frac{SQ}{\lambda}$$

(4)

where S is the sensitivity, Q is the quality factor, and λ is a resonant wavelength.

3. Sensor Design And Simulation Results

It was used a two-dimensional photonic crystal structure to create an interest biosensor. This structure includes dielectric rods in the air. In this structure, dielectric rods have the refractive index of 2.5 located in the air with the refractive index of 1 so that the number of 22 rods in the horizontal direction and that of 16 rods in the vertical direction were arranged. The lattice constant of this structure is equal to 600 nm, and the radius of insulation rods is equal to 120 nm. The simulation results show that a forbidden photonic band has been created for transverse electric (TE) and transverse magnetic (TM) modes of optical waves to calculate the proposed lattice band structure. Figure 1 depicts the band structure results.

To reach a biosensor using a two-dimensional photonic crystal structure, input and output pathways are required. Therefore, using linear defects, a pathway is created for an input that the input source is located at the beginning of pathway. A circle-shaped resonator is used between input and output to assign the resonant wavelength and filter other wavelengths. This resonator was created by a sort of rods in a circular form. This circle-shaped pathway was created to spread the light to the output in a resonant frequency.

One of the rods omitted in a resonator input causes the input frequency spectrum to decrease in the output and acts as a small resonator. On the other hand, it decreases the spectrum width in the output. In Fig. 2, the implemented structure can be seen.

In this structure, 36 rods were tested to be connected with a biosensor inside a nano-ring. But eventually, the rod $S13$ was selected as the best rod to be connected with the biosensor.

In the Figs. 3 to 16, the sensor output was depicted in terms of the refractive indices of blood ingredients, respectively. As you see in Table 1, the refractive index of blood ingredients connected to this rod, quality factor, sensitivity, detection limit, and finally FOM were depicted in this structure.

In Fig. 1, we can observe the sensor output without any biomolecule in the measure rod. The sensor output has a wavelength of 1.541 in the reference mode, and the full width is 0.4 in half of the background. The quality factor in this mode is equal to 3875.

In Fig. 4, the output sensor was depicted when blood plasma is connected to the measure rod $S13$. The output spectrum is in the wavelength range from 1.54–1.55, and its output power is approximately 0.3. The refractive index of blood plasma is equal to 1.35. Furthermore, its quality factor and sensitivity are 3875 and 14.14, respectively.

In Fig. 5, the output sensor against of Bovine-Serum-Albumin connection to the measure rod can be observed. The power of sensor output is equal to 0.8 when the biomolecule is connected to the measure rod. Furthermore, its wavelength is 1.542. The refractive index of Bovine-Serum-Albumin is equal to 1.47, and the full width is 0.3 in its half of the background. Its quality factor and sensitivity have obtained 5166 and 0.63, respectively.

In Fig. 6, the sensor output against the ethanol connection to a sensing hole can be seen. Its output power is approximately equal to 0.36 in the range from 1.542 to 1.55. The refractive index of ethanol is 1.36 as well as its quality factor and sensitivity are 1.11 and 3875, respectively, when ethanol is connected to the measure rod.

In Fig. 7, the sensor output can be seen when blood hemoglobin is connected to the measure rod $S13$. The refractive index of blood hemoglobin is 1.34, and the output power of sensor connected to the measure rod is equal to 0.45. The quality factor and sensitivity of which are 5166 and 0.88, respectively.

When polyacrylamide is connected to a measure rod, the sensor output is approximately equal to 0.72 in the wavelength range from 1.540 to 1.550. The refractive index of polyacrylamide is equal to 1.452 as well as its quality factor and sensitivity are 5166 and 0.66, respectively. Thus, the full width is equal to 0.3 in its half of the background (Fig. 8).

Sylgard184_Glucose has a refractive index of 1.4. When it is connected to the measure rod, the full width is 0.3 in its half of the background. Its wavelength is 1.542 as well as its quality factor and sensitivity are 5166 and 0.75, respectively. The output power of the sensor is approximately equal to 0.52 when the substance is connected to the measure rod (Fig. 9).

In Fig. 10, Urethame-Dimethacrylate was connected to the measure rod, and its output power is approximately equal to 0.8. The refractive index of this substance is 1.481, and the full length is 0.4 in its half of the background. The quality factor and sensitivity of this sensor are 3875 and 0.83, respectively.

One of the blood ingredients is water. The refractive index of water is equal to 1.33. The output power of this sensor per each water connection to the measure rod is equal to 0.32 in the wavelength of 1.542. The full length is 0.4 in its half of the background. The quality factor and sensitivity of that are 3875 and 1.2, respectively.

One of the other blood ingredients is Cypton. Its refractive index is equal to 1.34. The full length is 0.3 in its half of the background in the wavelength of 1.542. The power output of this sensor is approximately 0.28. The quality factor and sensitivity of that have obtained 5166 and 0.88, respectively.

In Fig. 13, all blood ingredients were depicted and compared with the reference mode. The wavelength of reference mode is 1.541, and other measured wavelengths are about 1.542. When a biomolecule is connected to a measure rod, it causes the resonant wavelength to be displaced. Moreover, the output power of the sensor was doubled, and this causes the sensor output to be easily detected.

In Table 1, all ingredients were addressed and compared. Parameters of this table include the wavelength, quality factor, sensitivity, detection limit, and FOM. According to the table, the resonant wavelength changes from the reference mode due to connecting the biomolecule with different refractive indices and creating a displacement. Moreover, the higher refractive index than 1 is, the more quality factor is. The sensitivity of substances such as blood plasma, ethanol, and water has the highest value. Therefore, these substances have the highest FOM. According to the table, the interest structure has a good optical limitation and the resonant nan-ring located between internal and external waveguides has the highest performance to boost the quality factor and displace the resonant wavelength. This sensor has a photonic crystal circular nano-ring which creates the proper optical interaction with the analyte.

Table 1
The output of the sensor per the connection of biomolecules to the measure rod $S13$.

Name	RI	$\Delta\lambda_{FWHM}$	Wavelength	Q-Farctor	Sensitivity	DL	FOM
Reference	1	0.4	1541	3875	-	-	-
Blood Plasma	1.35	0.4	1542	3875	1.14	0.03	2.86
Bovine-Serum-Albumin	1.47	0.3	1542	5166	0.63	0.04	2.11
Ethanol	1.36	0.4	1542	3875	1.11	0.03	2.78
Hemoglobin	1.34	0.3	1542	5166	0.88	0.03	2.94
Polyacrylamide	1.452	0.3	1542	5166	0.66	0.04	2.21
Sylgard184_Glucose	1.4	0.3	1542	5166	0.75	0.03	2.51
Urethame-Dimethacrylate	1.481	0.4	1542	3875	0.83	0.04	2.08
Water	1.33	0.4	1542	3875	1.2	0.03	3.01
Cypton	1.34	0.3	1542	5166	0.88	0.03	2.94

Therefore, in Table 2, the current structure can be compared with other similar work.

Table 2
Comparison with previous work.

Reference	Wavelength	Q-Farctor	Sensitivity nm/RIU	DL RIU^{-1}	FOM nm/RIU
[12]	1545–1565	2500	690	-	1400
[13]	1570–1610	262	-	0.002	-
[14]	-	5000	306.25	-	103
[15]	-	2066.44	546.72	1.44	-
[16]	-	19.82	74.5	-	-
This work	1542–1550	5166	1.14	0.04	2.94

Conclusion

In this paper, the blood ingredients were addressed by a photonic crystal biosensor. This sensor has a circular nano-ring between internal and external waveguides. This structure was designed to obtain the high resonant wavelength displacement, quality factor, and sensitivity when the biomolecules are

connected to a measure rod. One of the proper characteristics of this sensor is that it can assign multiple rods to sense a biomolecule. In the input of sensor, the coupling distance has increased because of the creation of a point defect. Hence, this causes the quality factor and resonant wavelength displacement to increase.

References

1. Vahdati, A., Parandin, F.: Antenna patch design using a photonic crystal substrate at a frequency of 1.6 THz. Wireless Pers. Commun. **109**, 2213–2219 (2019)
2. Parandin, F., Mahtabi, N.: Design of an ultra-compact and high-contrast ratio all-optical NOR gate. Opt. Quant. Electron. **53**, 666 (2021)
3. Farmani, A., Mir, A., Irannejad, M.: 2D-FDTD simulation of ultra-compact multifunctional logic gates with nonlinear photonic crystal. J. Opt. Soc. **36**, 811–818 (2019)
4. Parandin, F., Malmir, M.R., Naseri, M., Zahedi, A.: Reconfigurable all-optical NOT, XOR, and NOR logic gates based on two dimensional photonic crystals. Superlattices Microstruct. **113**, 737–744 (2018)
5. Saghaei, H., Zahedi, A., Karimzadeh, R., Parandin, F.: Line defects on photonic crystals for the design of all-optical power splitters and digital logic gates. Superlattices Microstruct. **110**, 133–138 (2017)
6. Parandin, F., Moayed, M.: Designing and simulation of 3-input majority gate based on two-dimensional photonic crystals. Optik **216**, 164930 (2020)
7. Olyaee, S., Seifouri, M., Mohebzadeh-Bahabady, A., Sardari, M.: Realization of all-optical NOT and XOR logic gates based on interference effect with high contrast ratio and ultra-compacted size, Opt Quant Electron (2018)
8. Parandin, F.: Ultra-compact terahertz all-optical logic comparator on GaAs photonic crystal platform. Opt. Laser Technol. **144**, 107399 (2021)
9. Parandin, F., Kamarian, R., Jomour, M.: Designing an Optical 1-bit comparator based on two-dimensional photonic crystals. Appl. Opt. **60**, 2275–2280 (2021)
10. Abdollahi, M., Parandin, F.: A novel structure for realization of an all-optical, one-bit half-adder based on 2D photonic crystals. J. Comput. Electron. **18**, 1416–1422 (2019)
11. Parandin, F., Malmir, M.R.: Reconfigurable all optical half adder and optical XOR and AND logic gates based on 2D photonic crystals. Opt. Quant. Electron. **52**, 56 (2020)
12. Karkhanehchi, M.M., Parandin, F., Zahedi, A.: Design of an all optical half-adder based on 2D photonic crystals. Photon Netw. Commun. **33**, 159–165 (2017)
13. Parandin, F., Kamarian, R., Jomour, M.: A novel design of all optical half-subtractor using a square lattice photonic crystals. Opt. Quant. Electron. **53**, 114 (2021)
14. Mehdizadeh, F., Soroosh, M.: H. Alipour-Banaei. Proposal for 4-to-2 optical encoder based on photonic crystals. IET Optoelectron. **11**(1), 29–35 (2016)
15. Parandin, F., Karkhanehchi, M.M., Naseri, M., Zahedi, A.: Design of a high bitrate optical decoder based on photonic crystals. J. Comput. Electron. **17**, 830–836 (2018)

16. Ouahab, I., Naoum, R.: A novel all optical 4×2 encoder switch based on photonic crystal ring resonators. Optik **127**, 7835–7841 (2016)
17. Parandin, F.: High contrast ratio all-optical 4 × 2 encoder based on two-dimensional photonic crystals. Opt. Laser Technol. **113**, 447–452 (2019)
18. Alipour, A., Farmani, A., Mir, A.: High sensitivity and tunable nanoscale sensor based on plasmon-induced transparency in plasmonic metasurface. IEEE Sens. J. **18**, 7047–7054 (2018)
19. Farmani, A., Mir, A.: Graphene sensor based on surface plasmon resonance for optical scanning. IEEE Photonics Technol. Lett. **31**, 643–646 (2019)
20. Emami Nejad, H., Mir, A., Farmani, A.: Supersensitive and tunable nano-biosensor for cancer detection. IEEE Sens. J. **19**, 4874–4881 (2019)
21. Mozaffari, M.H., Farmani, A.: On-chip single-mode optofluidic microresonator dye laser sensor. IEEE Sens. J. **20**, 3556–3563 (2020)
22. Ghanbari, A., Kashaninia, A., Sadr, A., Saghaei, H.: Supercontinuum generation for optical coherence tomography using magnesium fluoride photonic crystal fiber. Optik **140**, 545–554 (2017)
23. Ghoshal, S., Mitra, D., Roy, S.: Biosensors and biochips for nanomedical applications. Sens. ransducers J. **113**, 1–17 (2010)
24. Monosk, R., Stredansky, M., Sturdik, E.: Biosensors-classification, characterization and new trends. Acta Chim. Slovaca **5**, 109–120 (2012)
25. Olyaee, S., Dehghani, A.A.: Ultrasensitive pressure sensor based on point defect resonant cavity in photonic crystal. Sens. Lett. **11**, 1854–1859 (2013)
26. Olyaeea, S., Naraghi, A.: Design and optimization of index-guiding photonic crystal fiber gas sensor. Photon Sens. **3**, 131–136 (2013)
27. Olyaee, S., Seifouri, M., Karami, R.: Designing a high sensitivity hexagonal nano-cavity photonic crystal resonator for the purpose of seawater salinity sensing. Opt. Quant. Electron. **97**, 2–9 (2019)
28. Parandin, F., Heidari, F., Rahimi, Z., Olyaee, S.: Two-dimensional photonic crystal Biosensors: A review. Opt. Laser Technol. **144**, 107397 (2021)
29. Bohunicky, B., Mousa, S.A.: Biosensors: the new wave in cancer diagnosis, nanotechnology. Sci. Appl. **4**, 1–10 (2010)
30. Fan, X., White, I.M., Shopova, S.I., Zhu, H., Suter, J.D., Sun, Y.: Sensitive optical biosensors for unlabeled targets: A review. Anal. Chim. Acta **620**, 8–26 (2008)
31. Bohunicky, B., Mousa, S.A.: Biosensors: the new wave in cancer diagnosis. Nanatechnol. Sci Appl **4**, 1–10 (2011)
32. Olyaee, S., Naraghi, A., Ahmadi, V.: High sensitivity evanescentfield gas sensor based on modified photonic crystal fiber for gas condensate and air pollution monitoring. Optik **125**, 596–600 (2014)
33. Baqir, M.A., Farmani, A., Fatima, T., Raza, M.R., Shaukat, S.F., Mir, A.: Nanoscale, tunable, and highly sensitive biosensor utilizing hyperbolic metamaterials in the near-infrared range. Appl. Opt. **57**, 9447–9454 (2018)

34. Farmani, A., Mir, A., Bazgir, M., Zarrabi, F.B.: Highly sensitive nano-scale plasmonic biosensor utilizing Fano resonance metasurface in THz range: numerical study. Phys. E: LowDimensional Syst. Nanostruct. **104**, 233–240 (2018)
35. Olyaeea, S., Mohebzadeh-Bahabady, A.: Two-curve-shaped biosensor using photonic crystal nano-ring resonators. JNS **4**, 303–308 (2014)
36. Tavousi, A., Rakhshani, M.R., Mansouri-Birjandi, M.A.: High sensitivity label-free refractometer based biosensor applicable to glycated hemoglobin detection in human blood using all-circular photonic crystal ring resonators. Opt. Commun. **429**, 166–174 (2018)
37. Arunkumar, R., Suaganya, T., Robinson, S.: Design and analysis of 2D photonic crystal based biosensor to detect different blood components. Photonic Sens. **9**, 69–77 (2019)
38. Aly, A.H., Mohamed, D., Mohaseb, M.A., Abd El-Gawaad, N.S., Trabelsi, Y.: Biophotonic sensor for the detection of creatinine concentration in blood serum based on 1D photonic crystal. RSC Adv. **10**, 31765–31772 (2020)
39. Maache, M., Fazea, Y., Hassan, I.B., Alkahtani, A.A.: High-sensitivity capsule-shaped sensor based on 2D photonic crystals. Symmetry **12**, 1480 (2020)
40. Bijalwan, A., Singh, B.K., Rastogi, V.: Analysis of one-dimensional photonic crystal based sensor for detection of blood plasma and cancer cells. Optik **226**, 165994 (2020)

Figures

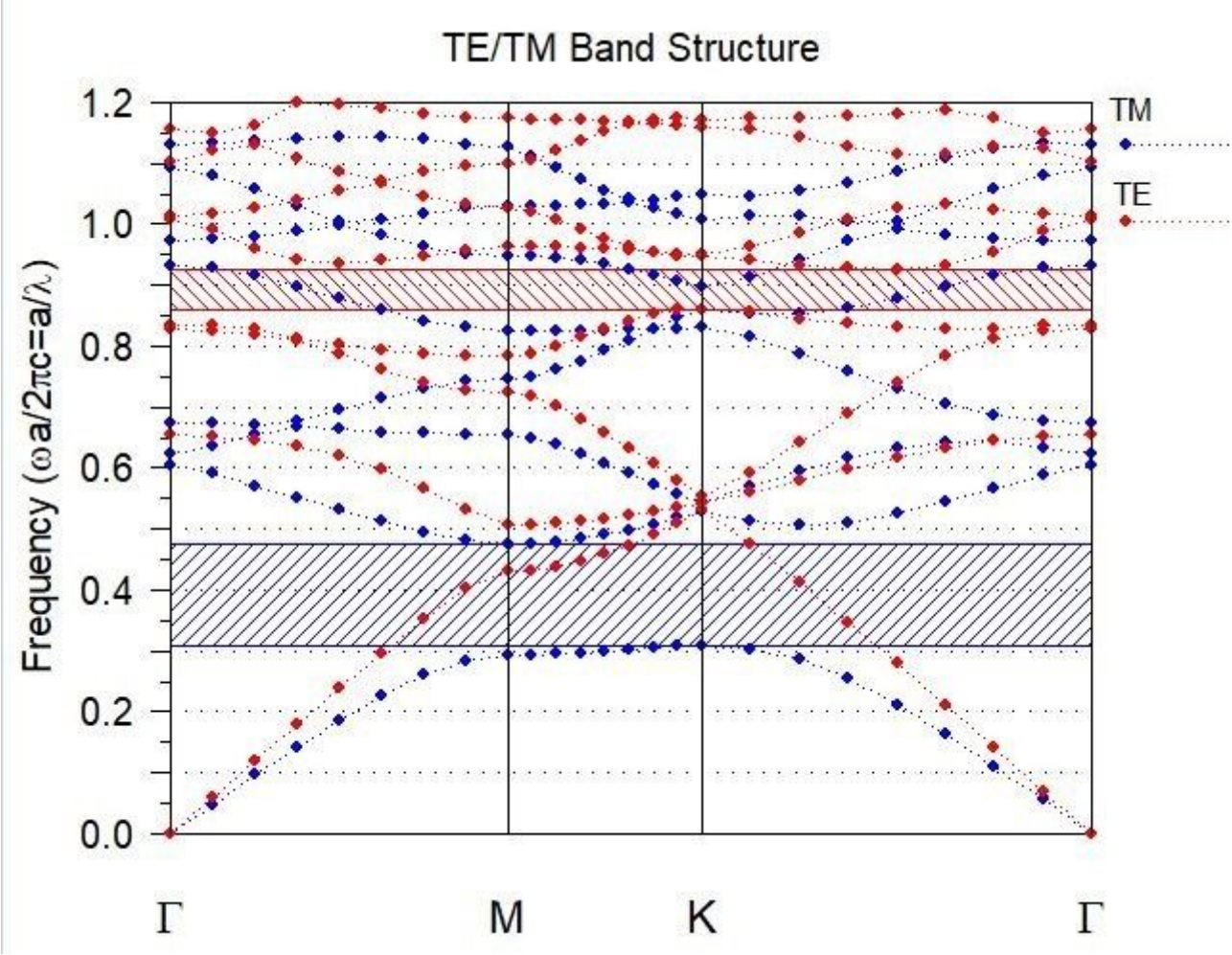

Figure 1

Calculation of TE and TM modes in a band structure

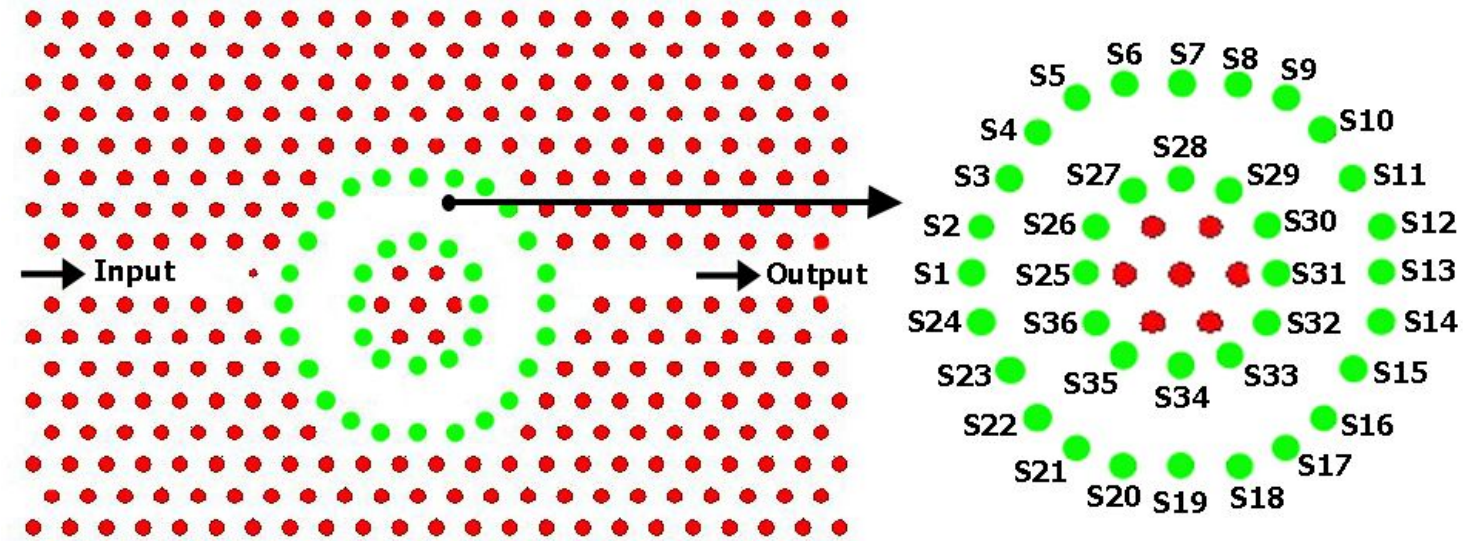

Figure 2

The designed sensor structure along with the measure rods

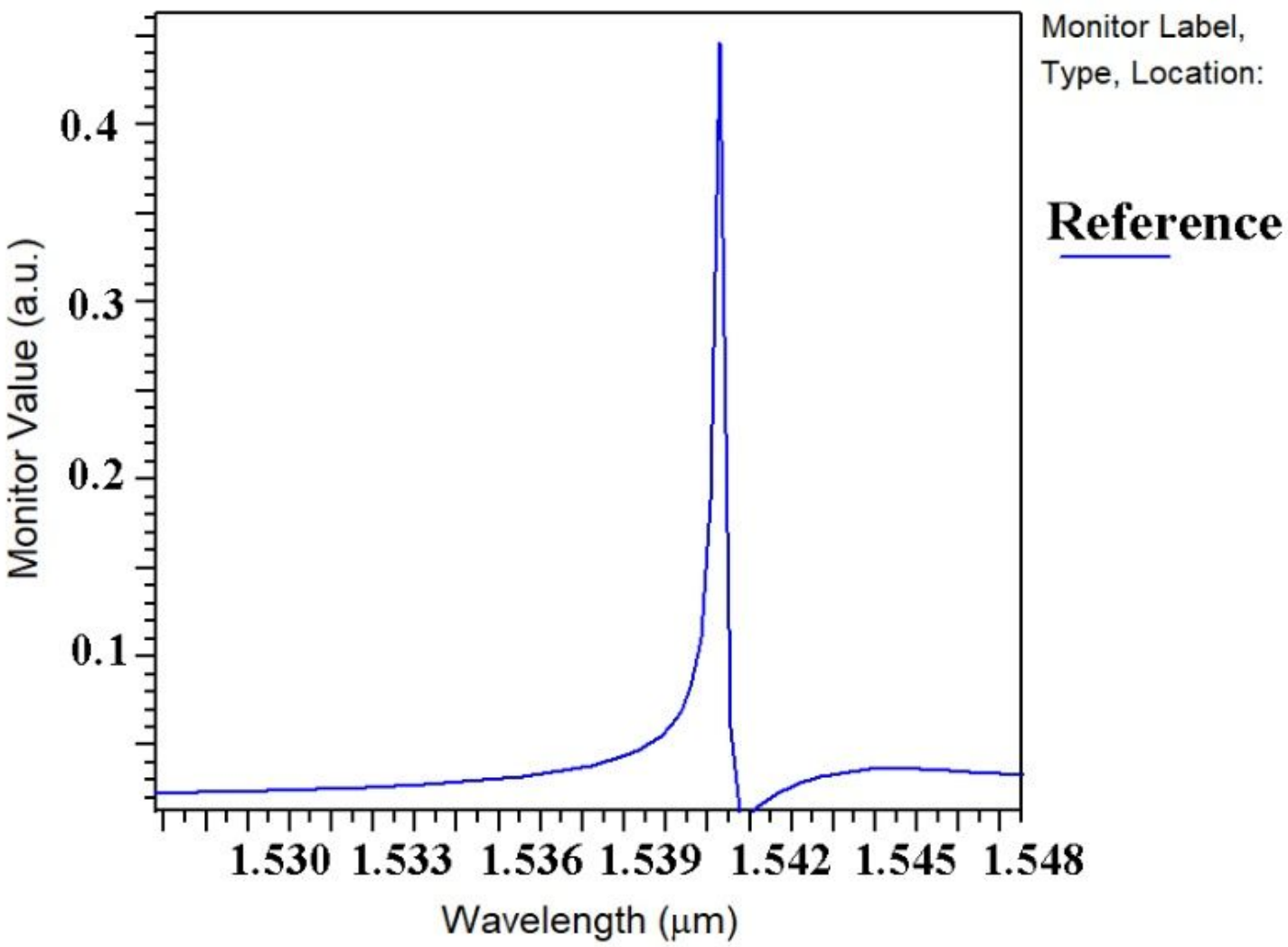

Figure 3

Sensor output in the reference mode without any biomolecule connection

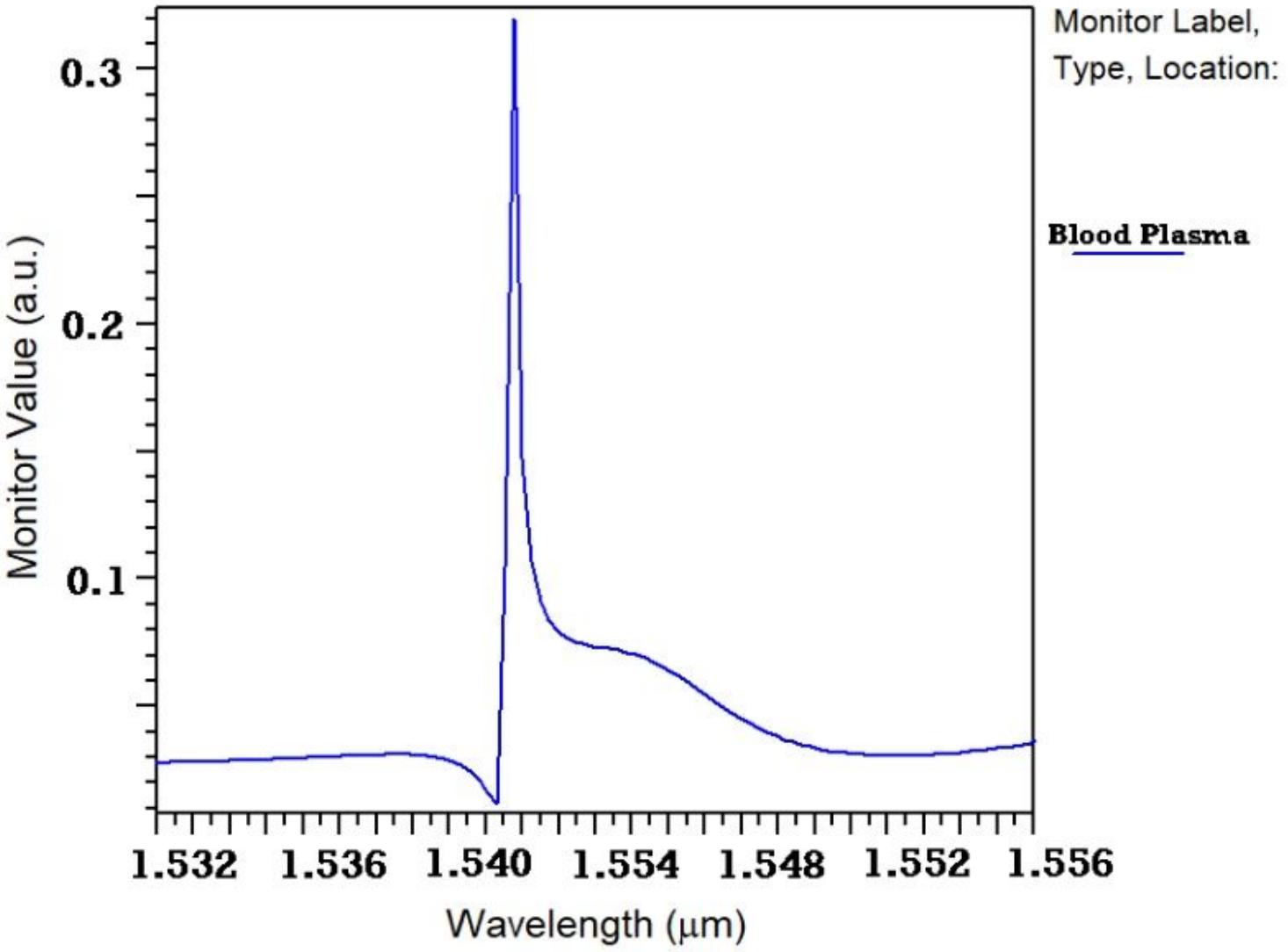

Figure 4

Sensor output for Blood Plasma

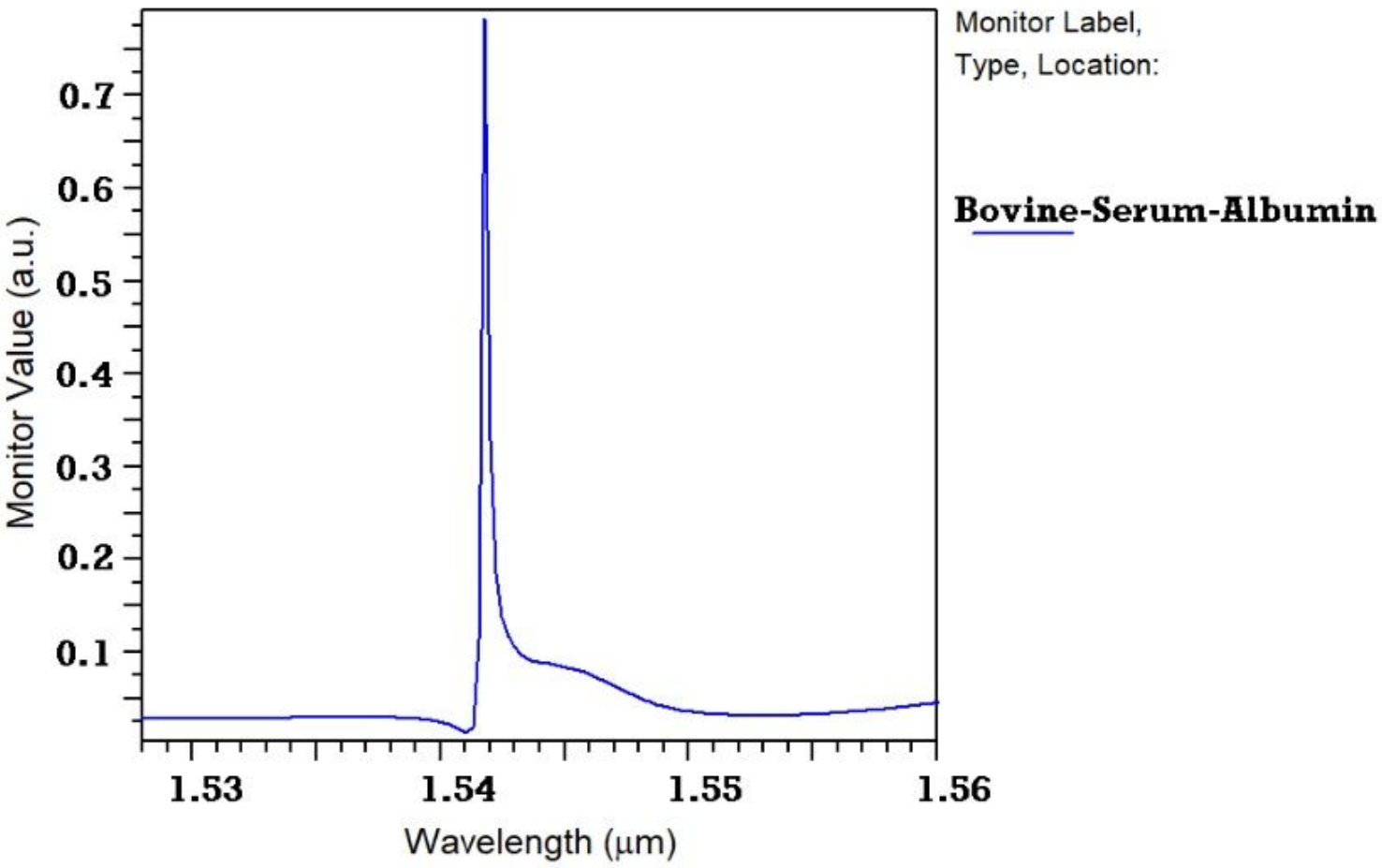

Figure 5

Sensor output for Bovine-Serum-Albumin

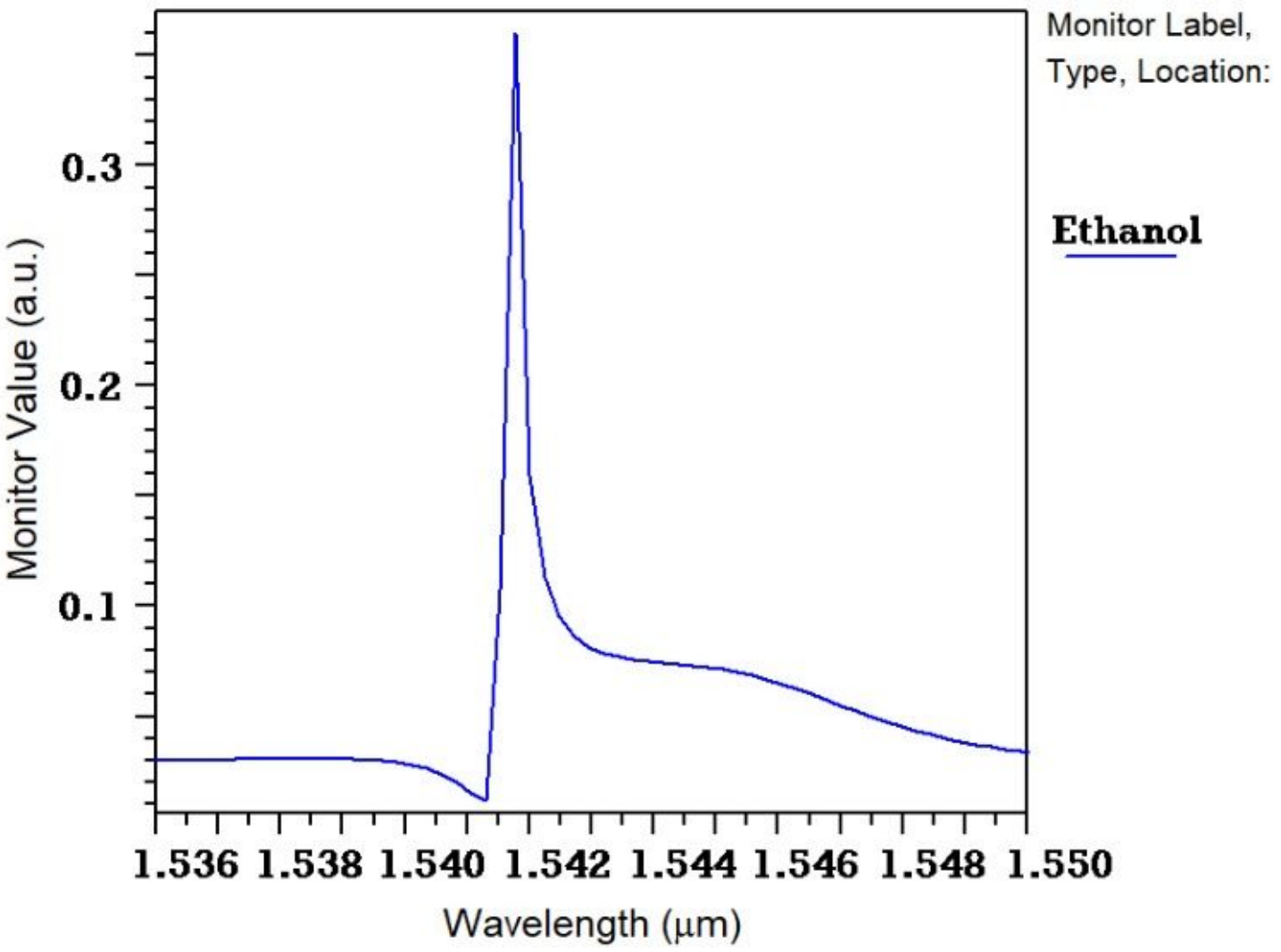

Figure 6

Sensor output for Ethanol

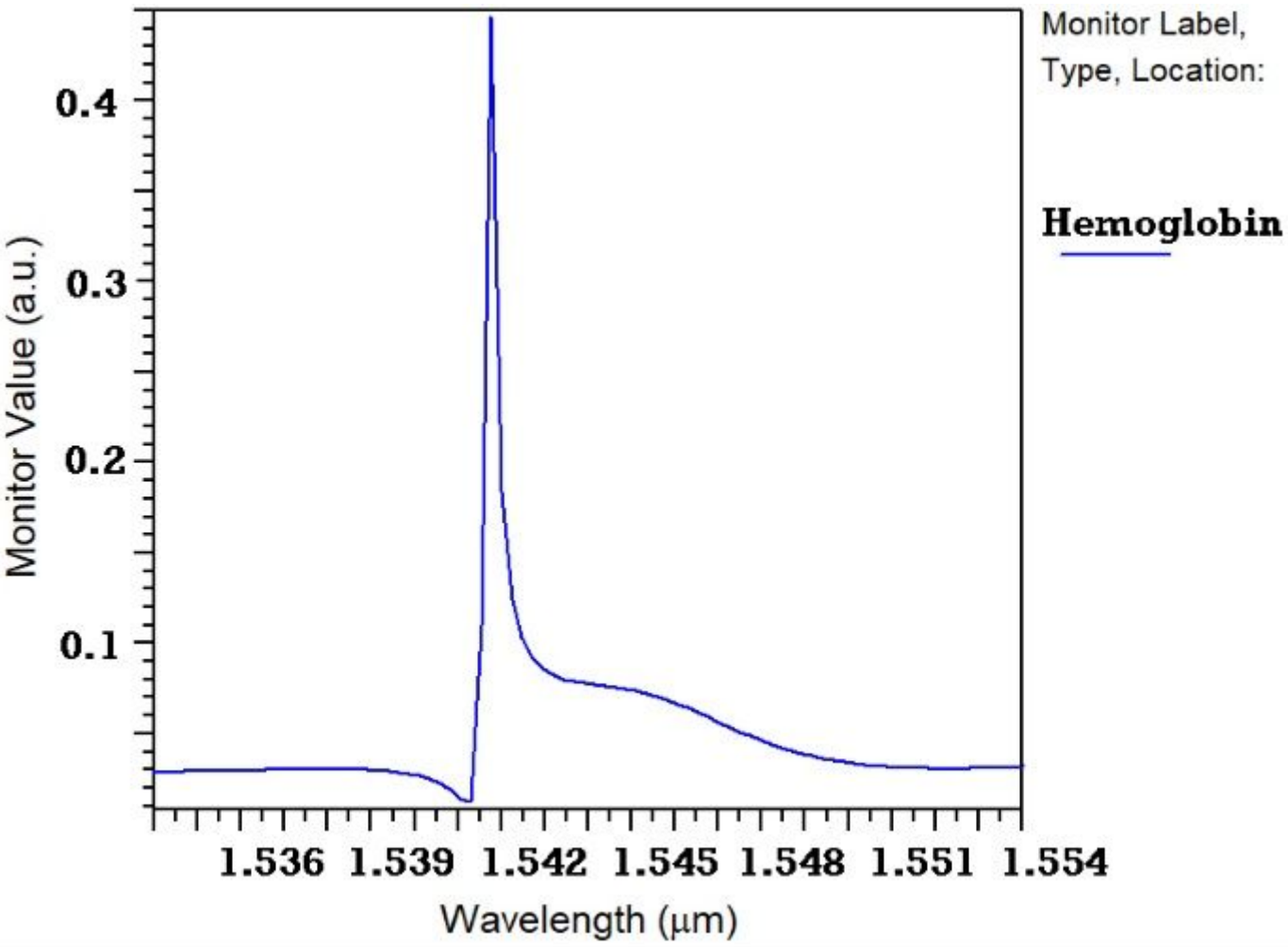

Figure 7

Sensor output for Hemoglobin

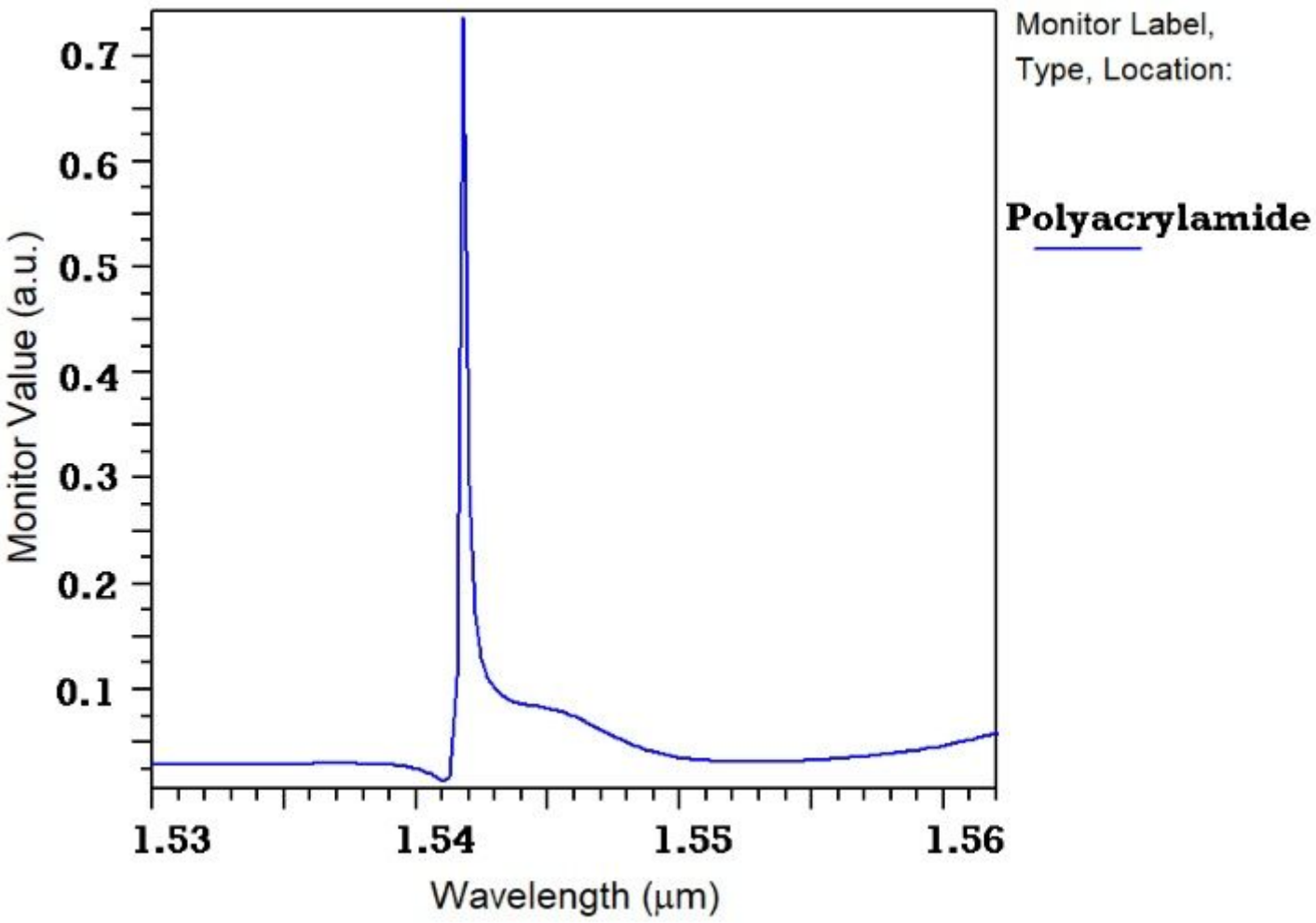

Figure 8

Sensor output for Polyacrylamide

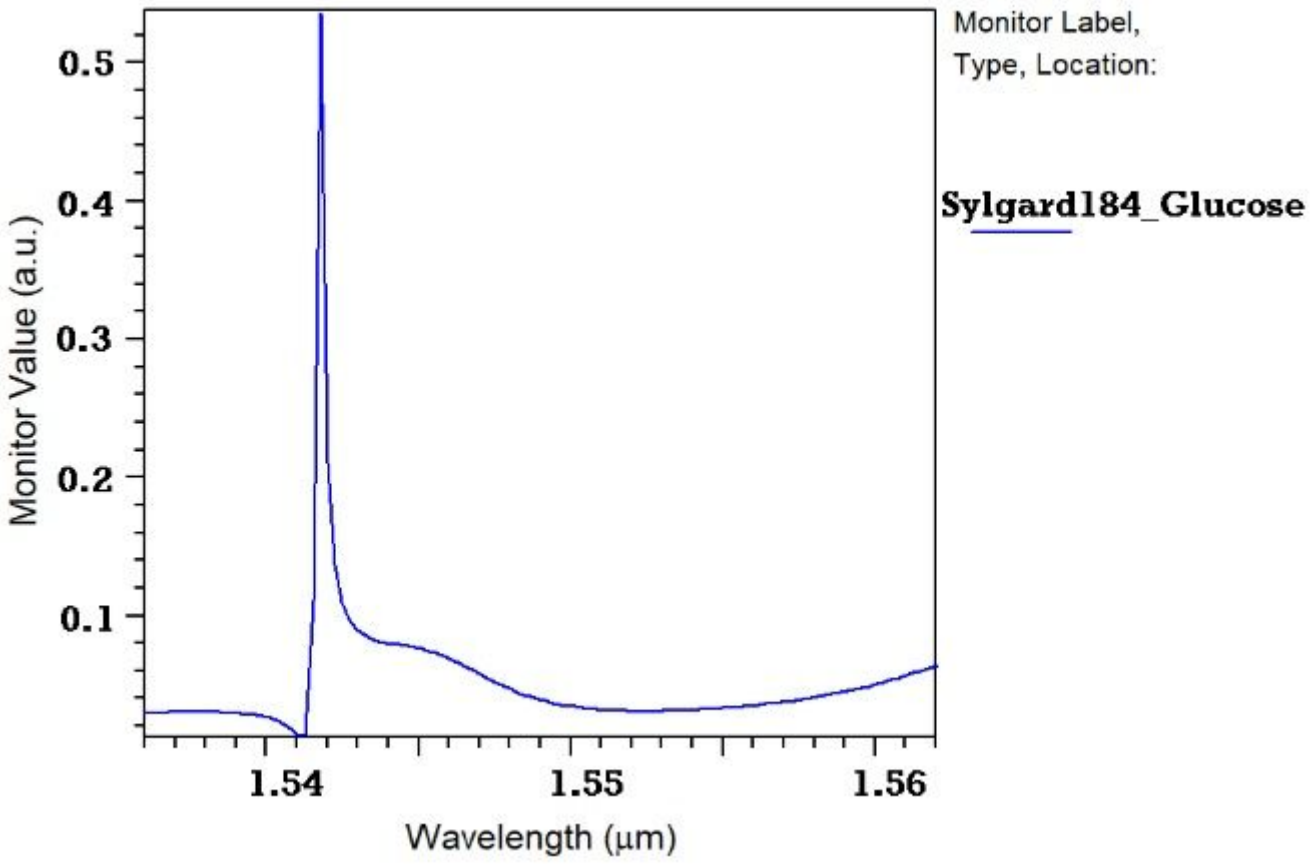

Figure 9

Sensor output for Sylgard184_Glucose

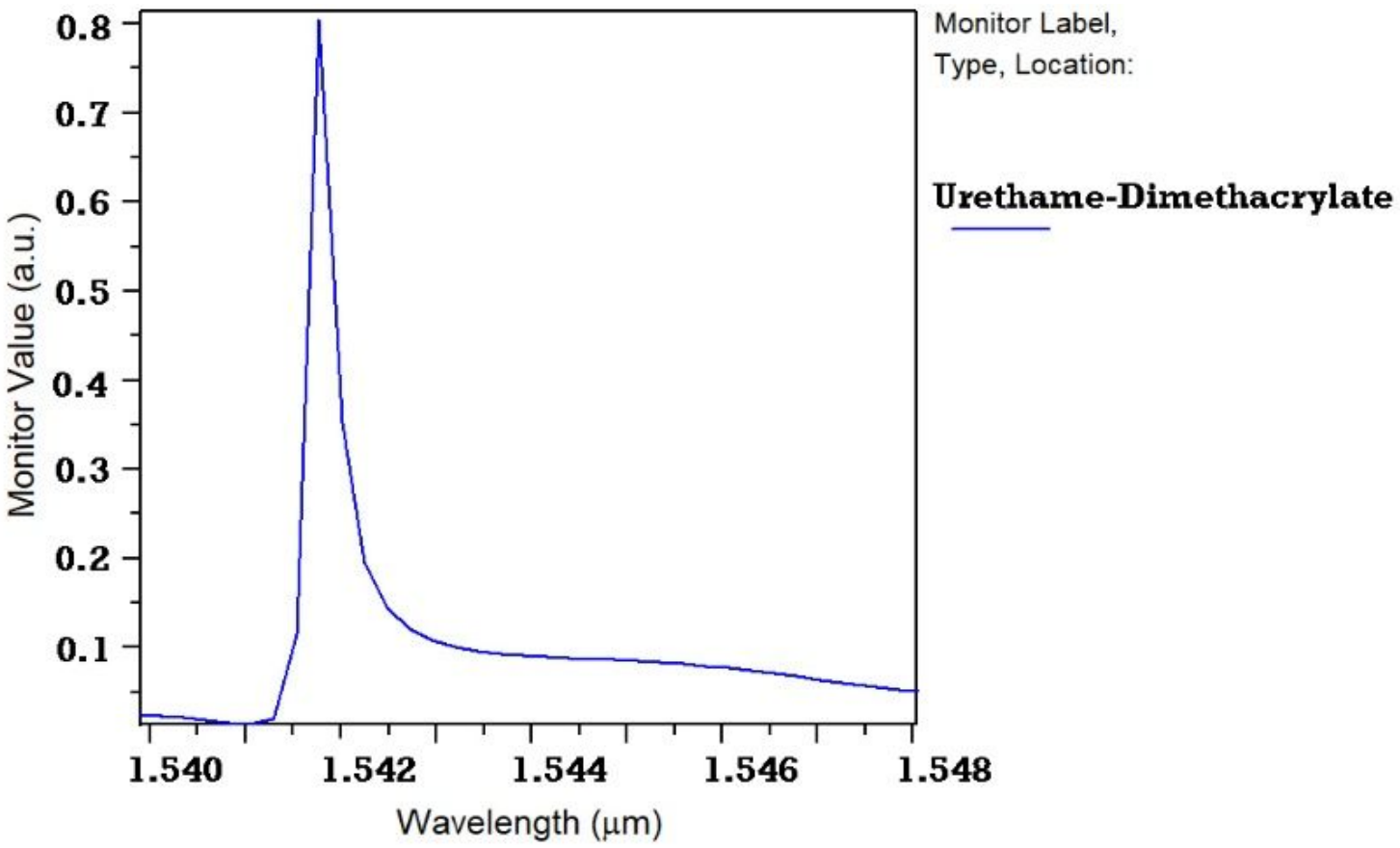

Figure 10

Sensor output for Urethame-Dimethacrylate

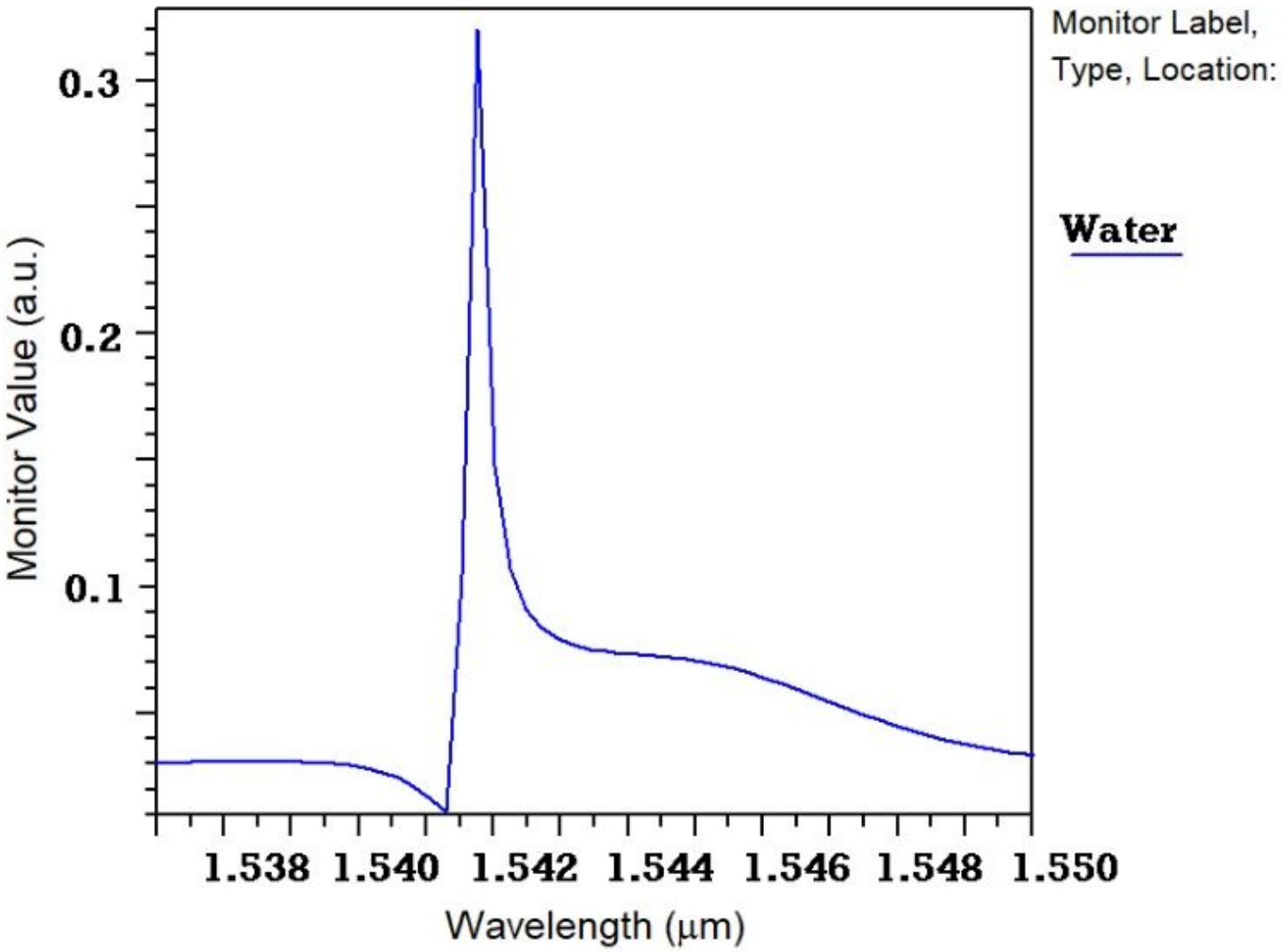

Figure 11

Sensor output for Water

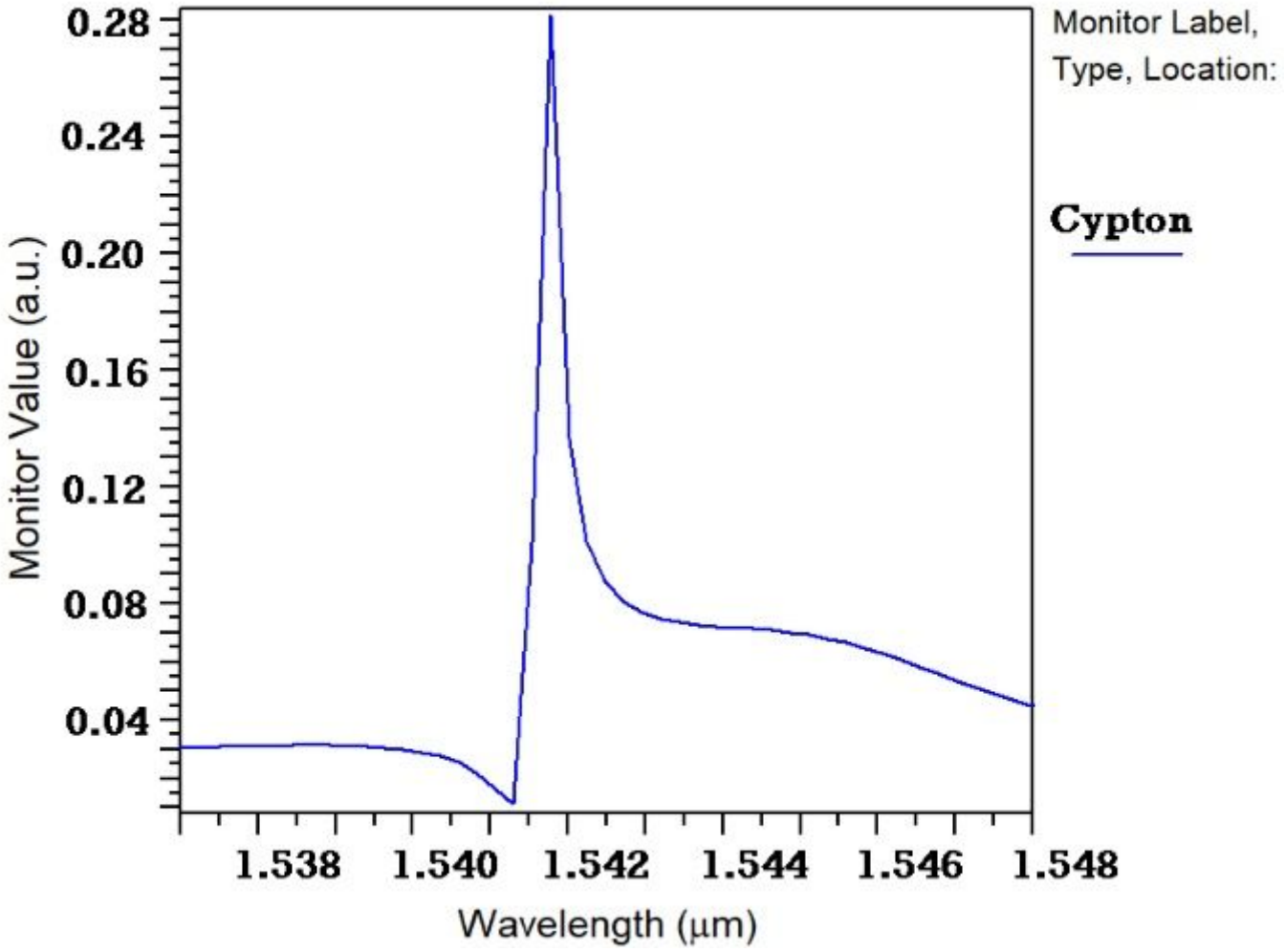

Figure 12

Sensor output for Cypton

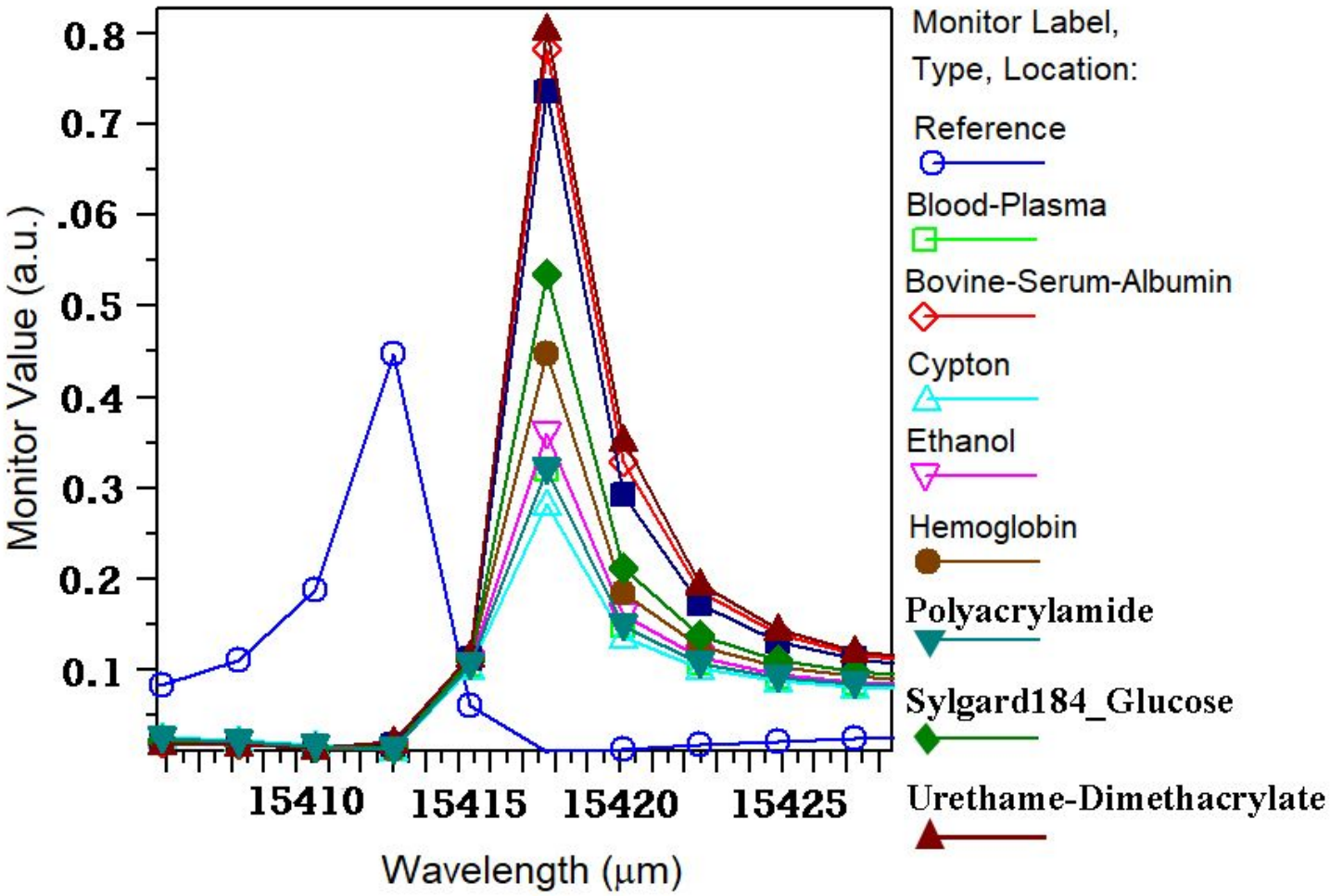

Figure 13

Output wavelength spectrum per different refractive indices of blood ingredients